Particle Filtering Based Track-before-detect Method for Passive Array Sonar Systems

Wei Yi[a,*], Lingzhi Fu[a], Ángel F. García-Fernández[b,c], Luxiao Xu[a], Lingjiang Kong[a]

[a]School of Information and Communication Engineering, the University of Electronic Science and Technology of China
[b]Department of Electrical Engineering and Electronics, University of Liverpool, Liverpool L69 3GJ, United Kingdom
[c]ARIES Research Center, Universidad Antonio de Nebrija, C\ Pirineos 55, Madrid 28015, Spain

Abstract

This work considers the underwater tracking of an unknown and time-varying number of targets, i.e., acoustic emitters, using passive array sonar systems. This problem becomes more challenging if the signal-to-noise ratio (SNR) of the acoustic emitter is low. To address this problem, a complete particle filter track-before-detect (PF-TBD) signal processing procedure is especially developed for the passive array sonar systems. Specifically, in order to enhance the detection performance of the low SNR targets, the unthresholded spectrum measurements after the beamforming of the acoustic signals are directly used as the inputs of the PF-TBD method. To better model the statistical characteristics of the spectrum measurements, a data fitting based parameter estimation algorithm is proposed to build accurate likelihood functions. Then the joint multi-target probability density (JMPD) can be recursively propagated forward by particle filtering to estimate the multi-target states. To accommodate the time-varying number of targets, the trajectory initiation and termination strategies are also integrated into the filtering process by adaptively adjusting the state dimensions of the JMPD at each measurement time. Finally, the efficacy of the proposed PF-TBD method is demonstrated both in simulation and on collected real-world data.

Keywords: Passive Array Sonar, Track-before-detect, Particle Filtering.

1. Introduction

Passive sonar array systems have attracted much attention in underwater detection and tracking due to their remarkable covertness, anti-jamming capability [1, 2], and also the particularity of propagation medium in the marine environment [2, 3]. In general, acoustic sensors are hull-mounted arrays and the common examples are towed linear arrays [4, 5] as is shown in Fig. 1. In the past years, acoustic source tracking with hydrophone array has been widely studied and applied in many important scenarios, such as underwater vehicle navigation, military defense and ocean biological signal analysis [2].

Since common passive array sonar systems can only provide bearing measurements, the underwater target tracking based on passive array sonar is usually formulated as bearing-only tracking (BOT) [6–9] problems. Correspondingly, a number of approaches have been proposed [10–14]. Such classical tracking methods adopt thresholded bearing measurements after detection process, which is known as detect-before-track (DBT) method. Exciting developments with DBT based underwater tracking have been advocated by various studies [15–21]. Specifically, a joint probabilistic data association filter (JPDAF) is implemented in sonar application, which updates each track with points weighted by the corresponding association probabilities [15]. In [16], the generalized Kalman filtering method is applied to underwater target tracking successfully. To reduce the tracking errors in BOT problem, a novel estimator is proposed through pre-processing the obtained bearings [17]. Moreover, because of the nonlinear relationship between bearing measurements and states of targets, particle filters (PFs) have also been applied in BOT problems [18, 19], especially for underwater acoustic target tracking [20–22], for its remarkable performance in nonlinear and non-Gaussian systems.

However, with the development of acoustic concealment technology [23], detecting and tracking targets with low signal-to-noise ratio (SNR) has become an urgent problem. The acoustic signals of interest are distorted by ambient noise and are more likely to be undetected using the conventional DBT method because much of the information contained in the measurements is irreversibly discarded after the thresholding process.

To address the target tracking problem in low SNR situations, track-before-detect (TBD) methods can be employed [24]. The main feature is that the tracker processes the entire raw measurements with intensities rather than just thresholded exceedances [25–27]. Recently, particle filter based track-before-detect (PF-TBD) for underwater multi-target tracking (MTT) has been studied [28–30]. Specifically, a Bayesian approach for multi-target tracking is implemented using bearing measurements [28], assuming both the number of targets and the form of likelihood distribution are known. To adapt the multi-path environments, an auxiliary PF-TBD method is proposed in [29], in which a robust multivariate Laplace distribution for likelihood is considered. More recently the investigations of PF-

*Corresponding author
Email address: kussoyi@gmail.com (Wei Yi)

[1]This work was supported in part by the Chang Jiang Scholars Program, in part by the National Natural Science Foundation of China under Grant 61771110.

TBD methods also includes other applications, such as speech source tracking [31] and passive bistatic radars (PBR) [32].

Due to the special characteristics and complexity of the underwater environment, the acoustic target tracking using passive array sonar is still a challenging task, especially when the target SNR is low. This work also considers the underwater acoustic target tracking problem and proposes a complete PF-TBD signal processing procedure. To enhance the tracking performance in low SNR environment, the unthresholded spectrum measurements after the beamforming of the acoustic signals are directly used as the inputs of the PF-TBD method. The important modules include frequency domain processing, the generation of bearing measurements, the particle filtering based propagation of the joint multi-target posterior density (JMPD) [33, 34], the data fitting based likelihood construction, and the trajectory initiation and termination modules. To the best of our knowledge, such a complete PF-TBD procedure especially developed for passive array sonar systems has not been seen in the existing relevant studies [25–29].

In order to better model the statistical characteristics of spectrum measurements, we propose a data fitting based estimation algorithm to build accurate likelihood functions. Existing PF-TBD methods applied in passive underwater tracking usually assume that the measurement likelihood function is known with a fixed form [28–30]. However, the practical underwater environment is complicated and changeable, simply assuming a specific likelihood model may not ensure an acceptable performance due to model mismatch between the actual statistical characteristics of real data and the assumed likelihood functions. We also remark that the random finite set (RFS) methods available in the literature with unknown likelihood [35–38] deal with MTT based on detections measurements, not the unthresholded raw measurements in TBD problem. In this paper, we use JMPD to perform target state estimation with multiple targets but the proposed approach could be used with RFS theory [2].

With the formulated likelihood function, then the JMPD can be propagated forward to recursively estimate the target states. Since the system models is highly non-linear and non-Gaussian, particle filtering is used to approximate the JMPD. Further, to accommodate the time-varying number of targets, the trajectory initiation and termination strategies are also integrated in the filtering process by adaptively updating the state dimensions of the JMPD at each measurement time.

In the simulation examples, we provide extensive performance studies of the proposed method, including the effect of three different beamforming methods and the performance comparison with the Kalman based DBT method [6, 8] and the Gaussian mixture probability hypothesis (PHD) filter [41]. Finally, the efficacy of the proposed method is tested on experimental data.

This work is an extension of a previous conference paper [30] with a more complete algorithm development and enhanced performance studies. The rest of the paper is organized in the following manner. The system models are given in Section 2. In Section 3, we develop a complete PF-TBD signal processing framework for passive array sonar systems, including frequency domain processing, generating of bearing measurements, particle filtering based propagation of JMPD, the data fitting based likelihood construction, and the trajectory initiation and termination modules. In Section 4, the efficacy of the proposed method is illustrated both in simulation and on collected real-world data. Finally, we draw the conclusions in Section 5.

[2]Note that, as [39], the JMPD could have written with RFS notation following the equivalences in [40].

2. System Models

2.1. Narrow-band Signal Model

The goal of this work is to derive an effective method to detect and track multiple moving acoustic emitters, especially in low SNR conditions, using a passive array system. At continuous time t, there are $L_t \geq 0$ acoustic emitters moving in the surveillance area, and sensed by a hydrophone array with M elements. The l-th, $l = 1, 2, \ldots, L_t$, acoustic emitter is located at bearing θ_l^t, moving with a bearing velocity $\dot{\theta}_l^t$ (in rad/s), and transmitting a narrow-band acoustic signal. Let $\mathbf{x}_l^t = [\theta_l^t \ \dot{\theta}_l^t]'$ denote the state of the l-th target at time t. Then, the multi-target state is the concatenation of the individual target states, namely $\mathbf{X}^t = \left[[\mathbf{x}_1^t]', [\mathbf{x}_2^t]', \ldots, [\mathbf{x}_{L_t}^k]'\right]'$ with $'$ denoting matrix transpose. We also denote the multi-target bearing vector as $\boldsymbol{\theta}^t = \left[[\theta_1^t], [\theta_2^t], \ldots, [\theta_{L_t}^t]\right]'$.

We assume that the emitters are in the far field of the array. As shown in Fig. 1, we consider a uniform linear array (ULA) system. Regarding the l-th acoustic emitter, the narrow-band signal received by the first element is denoted as $\tilde{y}_l^1(t) = s_l(t)e^{jw_l t} + v^1(t)$, where $s_l(t)$ is the complex envelope, ω_l denotes the carrier angular frequency of the received signal from the l-th emitter and $v^1(t)$ denotes the inevitable received additive noise. Then the corresponding signal received by the m-th, $m = 1, 2, \ldots, M$, element can be written as

$$\tilde{y}_l^m(t) = s_l(t - \tau^m(\theta_l^t))e^{j\omega_l(t-\tau^m(\theta_l^t))} + v^m(t), \tag{1}$$

where $\tau^m(\theta_l^t)$ denotes the propagation delay between the first and the m-th element, and $v^m(t)$ is the noise received by m-th element. For the linear array with elements separated by d, $\tau^m(\theta_l^t) = (m-1)\tau(\theta_l^t) = (m-1)d\sin\theta_l^t/c$, where c denotes the propagation speed of acoustic wave in water area and $\tau(\theta_l^t) = d\sin\theta_l^t/c$ represents the propagation time delay between each element. With respect to the assumption that the acoustic signal is narrow-band, the complex envelope $s_l(t)$ is slowing time-varying comparing to the carrier $e^{jw_l t}$. According to the standard narrow-band assumption in the array processing [42], the array aperture is much less than the inverse relation bandwidth. Then we can write

$$s_l(t) \approx s_l(t - \tau^m(\theta_l^t)), m = 1, 2, \cdots, M. \tag{2}$$

It means that the difference in complex envelope of signals received by each array element at the same sampling time can be ignored. Then (1) can be rewritten as

$$\tilde{y}_l^m(t) \approx s_l(t)e^{j\omega_l t}e^{-j\omega_l\tau^m(\theta_l^t)} + v^m(t). \tag{3}$$

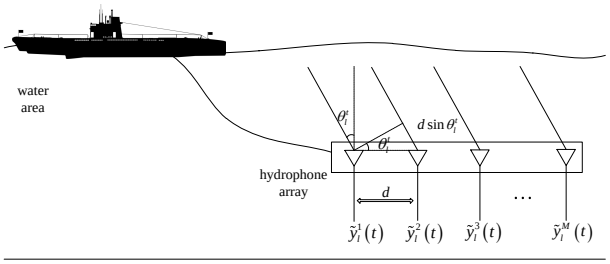

Figure 1: Model of signal received by a uniform linear array in a towed passive sonar system. The acoustic emitter at bearing θ_l^t is sensed by a hydrophone array with M elements separated by d.

Further define spatial phase as $\phi_l^t = \omega_l \tau(\theta_l^t)$, then the array output vector is modeled as

$$\tilde{\mathbf{y}}_l(t) = \mathbf{a}(\theta_l^t) s_l(t) e^{j\omega_l t} + \mathbf{v}(t), \tag{4}$$

where $\tilde{\mathbf{y}}_l(t) = [\tilde{y}_l^1(t)\ \tilde{y}_l^2(t)\ \dots\ \tilde{y}_l^M(t)]'$ denotes the received signal vector, $\mathbf{a}(\theta_l^t) = [1\ e^{-j\phi_l^t}\ \cdots\ e^{-j(M-1)\phi_l^t}]'$ denotes steering vector and $\mathbf{v}(t) = [v^1(t)\ v^2(t)\ \cdots\ v^M(t)]'$ is the noise vector. In general, the complex carrier $e^{j\omega_l t}$ does not carry any useful information and only complex baseband signals are considered [42]. Then, the discrete time complex baseband signal of (4) can be expressed as

$$\mathbf{y}_l(k) = \mathbf{a}(\theta_l^k) s_l(k) + \mathbf{v}(k), \tag{5}$$

where the discrete time variable k means the k-th sample time, namely time $t = k \cdot T$ with T the time interval between two consecutive time steps.

Next if we jointly consider the L_k acoustic emitters with incident angles $\theta_1^k, \theta_2^k, \cdots, \theta_{L_k}^k$, the matrix form of (5) can be expressed as [42],

$$\mathbf{y}(k) = \mathbf{A}(\boldsymbol{\theta}^k)\mathbf{s}(k) + \mathbf{v}(k), \tag{6}$$

where

$$\begin{aligned}\mathbf{A}(\boldsymbol{\theta}^k) &= [\mathbf{a}(\theta_1^k)\ \mathbf{a}(\theta_2^k)\ \cdots\ \mathbf{a}(\theta_{L_k}^k)] \\ &= \begin{bmatrix} 1 & 1 & \cdots & 1 \\ e^{-j\phi_1^k} & e^{-j\phi_2^k} & \cdots & e^{-j\phi_L^k} \\ \vdots & \vdots & \ddots & \vdots \\ e^{-j(M-1)\phi_1^k} & e^{-j(M-1)\phi_2^k} & \cdots & e^{-j(M-1)\phi_{L_k}^k} \end{bmatrix}\end{aligned} \tag{7}$$

denotes an $M \times L_k$ signal steering matrix and $\mathbf{s}(k) = [s_1(k)\ s_2(k)\ \cdots\ s_{L_k}(k)]'$ is the vector of the L_k discrete signals. Note that $\mathbf{v}(k)$ represents the vector of unknown additive noise, which is independent of the signal and represents the effect of undesired signals, such as thermal noise or interference from the underwater environment.

2.2. Sonar Measurement Model

A challenging aspect of underwater MTT using passive sonar arrays is the creation of a measurement function/pre-processing suitable for TBD implementation. Beamforming is a classic technique in array signal processing. A beamformer combines

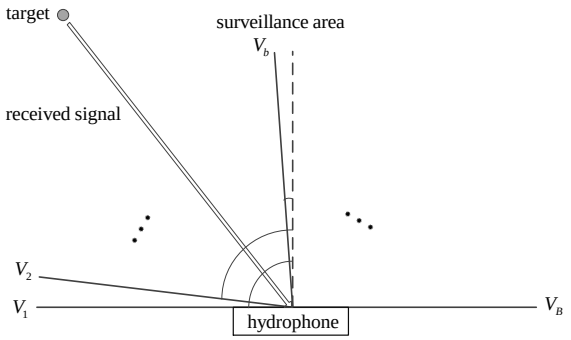

Figure 2: The surveillance area is divided into B bearing units.

the collected array data $\mathbf{y}(k)$ linearly with the beamforming weights, and enhances the signal from the desired spatial direction and reduces the signals from other directions. As shown in Fig. 2, we divide the surveillance area into B bearing cells denoted as $V_1, V_2, \cdots, V_B$ and the bearing resolution is determined by the array aperture Md. For the b-th ($b = 1, 2, \dots, B$) cell, the corresponding measurement z_b^k at time k is the beamformer output of that bearing direction after processing the received array signal $\mathbf{y}(k)$. The measurements of all bearing cells at time k are collected as $\mathbf{z}^k = \{z_b^k, b = 1, 2, \dots, B\}$. In addition, $\mathbf{Z}^{1:k}$ represents the received measurements up to time k, i.e., $\mathbf{Z}^{1:k} = \{\mathbf{z}^i, i = 1, 2, \cdots, k\}$. To keep as much as possible useful target information, the raw, unthresholded measurements $\mathbf{z}^k$ will be used as the inputs of the subsequent TBD algorithm. In principle, array data $\mathbf{y}(k)$ can also be used as the input of a TBD algorithm, but we use $\mathbf{z}^k$ as the input because it has a more direct relation with the target angle and, therefore, simplifies the processing chain.

Let $h(\cdot)$ denote a certain mapping function between the received array signal $\mathbf{y}(k)$ and the bearing measurement $\mathbf{z}^k$ after beamforming. For the direction cell V_b, its beamformer output z_b^k can be expressed as

$$z_b^k = h(\mathbf{y}(k), V_b). \tag{8}$$

Note that function $h(\cdot)$ directly affects the properties of the generated bearing measurement z_b^k. We propose and analyse three classical beamforming methods to determine function $h(\cdot)$ in Sections 3 and 4.

Given the multi-target state vector $\mathbf{X}^k$, measurements in each cell at this time step are assumed to be independent. For a multi-target state vector $\mathbf{X}^k$, let $V_b(\mathbf{X}^k) \geq 0$ denote the number of emitters transmitting signals in the b-th direction cell. The likelihood function can then be written as

$$p(\mathbf{z}^k|\mathbf{X}^k) = \prod_{b=1}^{B} \ell(z_b^k; V_b(\mathbf{X}^k)), \tag{9}$$

where $\ell(z_b^k; V_b(\mathbf{X}^k)$ denotes the measurement density for the b-th direction cell occupied by the $V_b(\mathbf{X}^k)$ targets. Note that the multi-target state $\mathbf{X}^k$ affects $\mathbf{z}^k$ by first affecting $\mathbf{y}(k)$ through (6), since the steering matrix $\mathbf{A}(\boldsymbol{\theta}^k)$ is the function of emitter

bearing angular. If $V_b(\mathbf{X}^k) = 0$, $\ell(z_b^k; V_b(\mathbf{X}^k) = 0)$ represents the measurement density of background noise and interference. If $V_b(\mathbf{X}^k) > 1$, it means there are more than one emitter transmitting signals in the b-th bearing direction. In that case, the signals from all the $V_b(\mathbf{X}^k)$ emitters will contribute to the b-th bearing measurement z_b^k after beamforming through (8). This will be seen more clearly in Section 3.2 where we will briefly review three classical beamforming methods.

Existing TBD works for underwater tracking usually assume that the measurement density $\ell(z_b^k; V_b(\mathbf{X}^k))$ is known with a specific form [28–30], e.g., Gaussian or Rayleigh distributed. However, the practical underwater environment is complicated and changeable. As indicated in (6), $\mathbf{v}(k)$ is the combination of the thermal noise and unknown interference from the underwater environment. Simply assuming a specific likelihood model may not ensure an acceptable performance due to model mismatch between the actual statistical characteristics of real data and the assumed likelihood functions. In Section 3.4, a data fitting based parameter estimation algorithm will be proposed to build an accurate form of $\ell(z_b^k; V_b(\mathbf{X}^k))$.

2.3. Emitter Motion Model

The emitters are assumed to move independently. Since the bearing motion of the underwater emitter is usually slow and with small maneuver, here we assume that the evolution of the states $p(\mathbf{x}_l^k|\mathbf{x}_l^{k-1})$ follows the nearly constant velocity (CV) motion model on the angular space and then the individual target evolves according to [6]

$$\mathbf{x}_l^k = \mathbf{F}\mathbf{x}_l^{k-1} + \mathbf{w}_l^k, \tag{10}$$

where $\mathbf{F}$ is the state-transition matrix given by

$$\mathbf{F} = \begin{bmatrix} 1 & T \\ 0 & 1 \end{bmatrix}, \tag{11}$$

where T denotes the time interval between two consecutive time steps and $\mathbf{w}_l^k$ is the process noise with covariance matrix

$$\mathbf{Q} = \kappa \times \begin{bmatrix} T^3/3 & T^2/2 \\ T^2/2 & T \end{bmatrix}, \tag{12}$$

where κ is the process noise intensity.

3. Algorithm Development

Based on the aforementioned models, we propose a complete PF-TBD signal processing procedure for underwater multi-target tracking in passive array sonar systems. The flowchart of this procedure is shown in Fig. 3. It can be seen that the input of the procedure is the wide-band array acoustic signal $\mathbf{y}(k)$ received by the hydrophones, and the output is the estimated multi-target state. The important steps include frequency domain processing, the generation of bearing measurements, the particle filtering based propagation of JMPD, the data fitting based likelihood construction, and the trajectory initiation and termination modules.

3.1. Frequency Domain Processing for the Wide-band Signal

The signal model in Section 2.1 is valid under the assumption that the signal is narrow-band. However, in practical passive sonar system, the received signals are usually wide-band [42]. If we consider the L_k wide-band acoustic signals $\mathbf{s}_w(k) = [s_1^w(k)\ s_2^w(k)\ \cdots\ s_{L_k}^w(k)]'$ with corresponding bearing $\theta_1^k, \theta_2^k, \cdots, \theta_{L_k}^k$. The received discrete time signal vector can be written as $\mathbf{y}_w(k) = [y_w^1(k)\ y_w^2(k)\ \cdots\ y_w^M(k)]'$, with signal received by the m-th, $m = 1, 2, \ldots, M$, array element expressed as

$$y_w^m(k) = \sum_{l=1}^{L_k} s_l^w(k - \tau^m(\theta_l^k)) + v_w^m(k), \tag{13}$$

where $v_w^m(k)$ denotes the unknown and wide-band additive noise. Note that approximation $s_l^w(k) \approx s_l^w(k - \tau^m(\theta_l^k))$ no longer holds for the wide-band model (13) as that for the narrow-band model in (1). To address this problem, frequency domain processing is adopted to split the received signal into several small frequency bins in frequency domain. The signals in each of these frequency bins can be treated as narrow-band signals which implies that the results in Section 2.1 can be applied.

In the following, we briefly introduce the steps for frequency segmenting. Consider the latest N snapshots of the received wide-band signal $\mathbf{y}_w(k)$. Divide the N snapshots into $\tilde{N}$ segments, each of which contains $Q = N/\tilde{N}$ snapshots. Perform the Q-point Fast Fourier Transform (FFT) in each segments and then the wide-band signal is decomposed into Q narrow-band signals with non-overlapping frequencies.

Based on the narrow-band results in Section 2.1, the frequency domain expression of the narrow-band signal for the q-th, $q = 1, 2, \cdots, Q$, frequency bin of the $\tilde{n}$-th, $\tilde{n} = 0, 1, \ldots, \tilde{N} - 1$, segment is,

$$y_w^m(f_q, \tilde{n}) = \sum_{l=1}^{L_k} a^m(f_q, \theta_l^k) s_l^w(f_q, \tilde{n}) + v_w^m(f_q, \tilde{n}). \tag{14}$$

where $s_l^w(f_q, \tilde{n})$ and $v_w^m(f_q, \tilde{n})$ denote, respectively, the signal and noise frequency intensities, and $a^m(f_q, \theta_l^k) = e^{-j(M-1)\phi_l^k(f_q)}$ with $\phi_l^k(f_q) = 2\pi f_q d \sin\theta_l^k / c$. Similar to the results of the narrow-band model in Section 2.1, the vector form of (14) can be expressed as

$$\mathbf{y}_w(f_q, \tilde{n}) = \mathbf{A}(f_q, \boldsymbol{\theta}^k)\mathbf{s}_w(f_q, \tilde{n}) + \mathbf{v}_w(f_q, \tilde{n}). \tag{15}$$

where

$$\begin{aligned}
\mathbf{y}_w(f_q, \tilde{n}) &= [y_w^1(f_q, \tilde{n})\ y_w^2(f_q, \tilde{n})\ \cdots\ y_w^M(f_q, \tilde{n})]' \\
\mathbf{s}_w(f_q, \tilde{n}) &= [s_1^w(f_q, \tilde{n})\ s_2^w(f_q, \tilde{n})\ \cdots\ s_L^w(f_q, \tilde{n})]' \\
\mathbf{v}_w(f_q, \tilde{n}) &= [v_w^1(f_q, \tilde{n})\ v_w^2(f_q, \tilde{n})\ \cdots\ v_w^M(f_q, \tilde{n})]' \\
\mathbf{A}(f_q, \boldsymbol{\theta}^k) &= [\mathbf{a}(f_q, \theta_1^k)\ \mathbf{a}(f_q, \theta_2^k)\ \cdots\ \mathbf{a}(f_q, \theta_L^k)] \\
\mathbf{a}(f_q, \theta_l^k) &= [1,\ a^2(f_q, \theta_l^k),\ \cdots,\ a^M(f_q, \theta_l^k)]'.
\end{aligned} \tag{16}$$

Further, based on the received signal snapshots, the correlation matrix of the received signal at frequency f_q can be approximately estimated by time averaging as [42]

$$\hat{\mathbf{R}}(f_q) = \frac{1}{\tilde{N}} \sum_{\tilde{n}=1}^{\tilde{N}} \mathbf{y}_w(f_q, \tilde{n})(\mathbf{y}_w(f_q, \tilde{n}))^H. \tag{17}$$

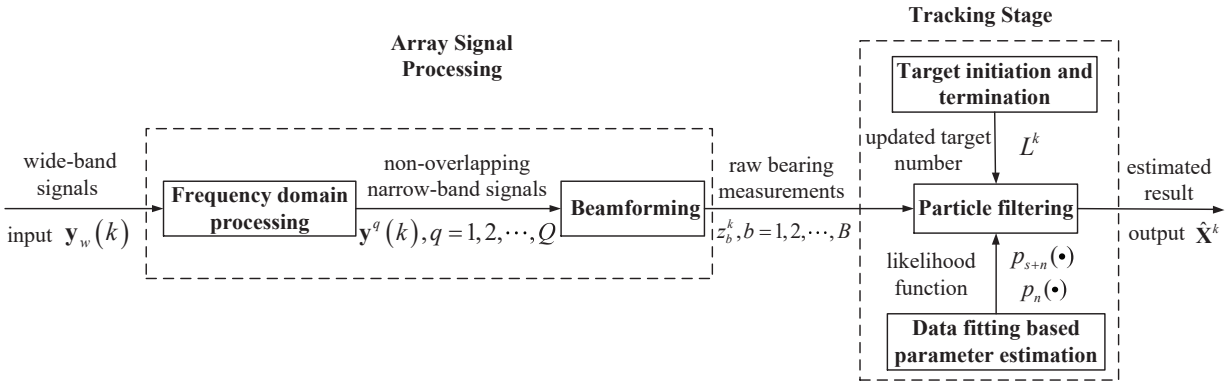

Figure 3: Architecture of the proposed PF-TBD. It consists two block diagrams, i.e., array signal processing for raw bearing measurements generating and PF stage for state estimation.

The estimated correlation matrix $\hat{\mathbf{R}}(f_q)$ describes the statistical characteristics of the underwater environment at frequency f_q, and will be used in the subsequent beamforming process.

Once the wide-band signal is decomposed into Q narrow-band signals, then the information from different frequency segments can be combined for further signal processing through the incoherent signal-subspace method (ISM) [43] or coherent signal-subspace method (CSM) [44].

3.2. Bearing Measurements Generation

The common approach to carry out space-time processing of array signals is beamforming [42, 45], in which the signal received by the hydrophones is delayed and added together with proper coefficient. Here, we adopt the ISM method [43] to solve the beamforming problem for the wide-band signal. Its main idea is to first perform narrow-band beamforming for each frequency bin separately, then sum up the power spectrums of all frequency bin incoherently. To study the impact of different bearforming methods on the subsequent tracking performance, we give the specific forms of the function $h(\cdot, V_b)$ in (8) for three classical beamformers.

3.2.1. Conventional beamforming (CBF)

CBF is a common spectral analysis method, which shows superior performance in isotropic and homogeneous noise [46]. As mentioned in Section 2.2, the unthresholded outputs of CBF are directly used in the subsequent TBD processing.

Given the received wide-band signal $\mathbf{y}_w(k)$, the outputted measurement at bearing V_b is the summation of the overall power of all Q frequency bins,

$$z_b^k = h_{\mathrm{CBF}}(\mathbf{y}_w(k), V_b) = \sum_{q=1}^{Q} P_{\mathrm{CBF}}(\mathbf{y}_w(f_q, k), V_b), \tag{18}$$

where $P_{\mathrm{CBF}}(\mathbf{y}_w(f_q, k), V_b)$ the power spectrum of the q-th frequency bins for bearing cell V_b is given by [46],

$$\begin{aligned} P_{\mathrm{CBF}}(\mathbf{y}_w(f_q, k), V_b) &= (\mathbf{a}(f_q, V_b))^H \\ &\quad \times \mathbb{E}[\mathbf{y}_w(f_q, k)(\mathbf{y}_w(f_q, k))^H]\mathbf{a}(f_q, V_b) \\ &= (\mathbf{a}(f_q, V_b))^H \hat{\mathbf{R}}(f_q)\mathbf{a}(f_q, V_b), \end{aligned} \tag{19}$$

where $\mathbb{E}(\cdot)$ denotes the statistical expectation, the superscript $(\cdot)^H$ is the conjugate transpose, and $\mathbf{a}(f_q, V_b)$ denotes the weight vector for the bearing V_b.

3.2.2. Minimum variance distortionless response (MVDR)

MVDR is a high resolution beamforming algorithm [47]. It keeps the signal of observation direction without distortion, while minimizes the average power of output signal. Thus, the direction observation of other signals is inhibited and the signal-to-noise ratio of the array output is maximized.

The outputted measurement of MVDR at bearing V_b is also the summation of the overall power of all Q frequency bins,

$$z_b^k = h_{\mathrm{MVDR}}(\mathbf{y}_w(k), V_b) = \sum_{q=1}^{Q} P_{\mathrm{MVDR}}(\mathbf{y}_w(f_q, k), V_b), \tag{20}$$

with $P_{\mathrm{MVDR}}(\mathbf{y}_w(f_q, k), V_b)$ the power spectrum output of the q-th frequency bins for bearing cell V_b, and can be calculated as,

$$P_{\mathrm{MVDR}}(\mathbf{y}_w(f_q, k), V_b) = \frac{1}{(\mathbf{a}(f_q, V_b))^H \hat{\mathbf{R}}(f_q)^{-1} \mathbf{a}(f_q, V_b)}. \tag{21}$$

3.2.3. Multiple signal classification (MUSIC)

The above two algorithms are based on the power of the output signal. The core of MUSIC is to decompose the covariance matrix of input data, and construct the signal subspace and the noise subspace with the eigenvectors [48]. Then, the spectrum can be constructed according to the orthogonality of these two subspaces.

The outputted measurement of MUSIC at bearing V_b is the summation of the outputs of all Q frequency bins,

$$z_b^k = h_{\mathrm{MUSIC}}(\mathbf{y}_w(k), V_b) = \sum_{q=1}^{Q} P_{\mathrm{MUSIC}}(\mathbf{y}_w(f_q, k), V_b), \tag{22}$$

with $P_{\mathrm{MUSIC}}(\mathbf{y}_w(f_q,k),V_b)$ the output of the q-th frequency bins for bearing cell V_b, and is constructed as

$$P_{\mathrm{MUSIC}}(\mathbf{y}_w(f_q,k),V_b) = \frac{1}{(\mathbf{a}(f_q,V_b))^H\hat{\mathbf{G}}(f_q)(\hat{\mathbf{G}}(f_q))^H\mathbf{a}(f_q,V_b)} \tag{23}$$

where $\hat{\mathbf{G}}(f_q)$ denotes the noise subspace obtained by calculating the eigenvalue decomposition of $\hat{\mathbf{R}}(f_q)$ [48]. Note that the outputted result by MUSIC is not a true spectrum, and is usually called a pseudo spectrum.

Overall, the mapping function $h(\cdot,V_b)$ mentioned in (8) is implemented by array signal processing and the bearing measurement at the cell V_b is generated. Calculate the bearing measurements of all units $V_1 \sim V_B$, the spectrum measurement frame of time k are generated, i.e., $\mathbf{z}^k=[z_1^k,\ldots,z_B^k]$. Then sort the spatial spectrum in chronological order, the bearing-time record (BTR), i.e., $\mathbf{Z}^{1:k}$, is generated which is the standard method to display sonar data.

3.3. Particle Filter based Multi-target Tracking

The aim of this section is to estimate the multi-target state $\mathbf{X}^k=\left[[\mathbf{x}_1^k]',[\mathbf{x}_2^k]',\ldots,[\mathbf{x}_{L_k}^k]'\right]'$, which implicitly includes an estimate of the number L_k of targets, based on the unthresholded beamformer outputs $\mathbf{Z}^{1:k}$. From a Bayesian perspective, this can be done by recursively calculating the posterior density function $p(\mathbf{X}^k|\mathbf{Z}^{1:k})$, i.e., the joint multiple probability density (JMPD) [33, 34]. In principle, the JMPD can be obtained in two stages: prediction and update.

Suppose that the JMPD $p(\mathbf{X}^{k-1}|\mathbf{Z}^{1:k-1})$ at time $k-1$ is available. The prediction stage involves with the motion model (10) and the Chapman-Kolmogorov equation

$$p(\mathbf{X}^k|\mathbf{Z}^{1:k-1}) = \int p(\mathbf{X}^k|\mathbf{X}^{k-1})p(\mathbf{X}^{k-1}|\mathbf{Z}^{1:k-1})d\mathbf{X}^{k-1}, \tag{24}$$

where $p(\mathbf{X}^k|\mathbf{X}^{k-1}) = \prod_{l=1}^{L_k} p(\mathbf{x}_i^k|\mathbf{x}_i^{k-1})$ is the evolution of the multi-target state defined by the motion model (10). Then, the update equation can be obtained via Bayes' rule

$$p(\mathbf{X}^k|\mathbf{Z}^{1:k}) = \frac{p(\mathbf{z}^k|\mathbf{X}^k)p(\mathbf{X}^k|\mathbf{Z}^{1:k-1})}{p(\mathbf{z}^k|\mathbf{Z}^{1:k-1})}, \tag{25}$$

where $p(\mathbf{z}^k|\mathbf{X}^k)$ is the likelihood function defined in (9), and $p(\mathbf{z}^k|\mathbf{Z}^{1:k-1})$ is the normalized constant.

Since the system models are non-linear and non-Gaussian, particle filter [49] is adopted to approximately estimate the JMPD. The key idea is to approximate the required JMPD by a set of weighted samples drawn sequentially from an importance density. Assume the availability of evenly weighted samples $\{\mathbf{X}_j^k\}_{j=1}^{N_p}$, where integer N_p denotes the sample size, representing the posterior at time $k-1$. In MTT context, the multi-target particles are partitioned into multiple partitions as $\mathbf{X}_j^k=\left[[\mathbf{x}_{1,j}^k]',[\mathbf{x}_{2,j}^k]',\ldots,[\mathbf{x}_{L_k,j}^k]'\right]'$, and the l-th partition $\{\mathbf{x}_{l,j}^k\}_{j=1}^{N_p}$ holds the corresponding sub-particles for the l-th target.

Following [50], assume posterior independence between each target at time $k-1$ and applying Bayes rule, the JMPD at time k can be approximately expressed as

$$p(\mathbf{X}^k|\mathbf{Z}^{1:k}) \propto p(\mathbf{z}^k|\mathbf{X}^k)\prod_{l=1}^{L_k}\sum_{j=1}^{N_p} p(\mathbf{x}_l^k|\mathbf{x}_{l,j}^{k-1}). \tag{26}$$

The analysis in [50] shows that assuming the above posterior independence can provide a better Monte Carlo approximation of the prior distribution at the next time, and therefore the posterior at the next time, independently of the sampling method is performed.

By employing the idea of the auxiliary particle filter [51], drawing samples from (26) can be equally achieved by sampling from the higher dimensional joint density

$$p(\mathbf{X}^k,\mathbf{u}|\mathbf{Z}^{1:k}) \propto p(\mathbf{z}^k|\mathbf{X}^k)\prod_{l=1}^{L_k} p(\mathbf{x}_l^k|\mathbf{x}_{l,u_l}^{k-1}). \tag{27}$$

where the vector $\mathbf{u}=[u_1,\ldots,u_{L_k}]$ of auxiliary variables are indices on the samples at the previous time [34, 50, 51]. To be specific, u_l is the index of the sample from which the lth target will be propagated. The auxiliary variables aid in the sampling of suitable values of the multi-target state $\mathbf{X}^k$, and are discarded after the sampling procedure is completed.

Multi-target state $\mathbf{X}_j^k$ and vector $\mathbf{u}_j$ are drawn, for $j=1,\ldots,N_p$, from an importance density $q(\cdot)$ and weighted as

$$\omega_j^k \propto \frac{p(\mathbf{z}^k|\mathbf{X}_j^k)\prod_{l=1}^{L_k} p(\mathbf{x}_{l,j}^k|\mathbf{x}_{l,u_{l,j}}^{k-1})}{q(\mathbf{X}_j^k,\mathbf{u}_j|\mathbf{Z}^{1:k})}, \tag{28}$$

Finally, normalization is applied to ensure the summation of weights is one. By designing different importance densities $q(\cdot)$, various particle filters for MTT have been proposed [33, 34, 39, 50]. Here we adopt the parallel partition particle filter method [39], since it is computationally efficient and can provide good tracking performance when targets are in close proximity. In this case, the importance density has the following expression,

$$q(\mathbf{X}^k,\mathbf{u}|\mathbf{Z}^{1:k}) \propto \prod_{l=1}^{L_k} p(\mathbf{z}^k|\hat{\mathbf{X}}_{\{1,\ldots,L_k\}/l}^k,\mathbf{x}_l^k)p(\mathbf{x}_l^k|\mathbf{x}_l^{k-1,u_l}) \tag{29}$$

where $\hat{\mathbf{X}}_{\{1,\ldots,L_k\}/l}^k$ denotes the estimated target states of all except the lth target, and is obtained by averaging the predicted states over all the particles. The multi-target likelihood $p(\mathbf{z}^k|\hat{\mathbf{X}}_{\{1,\ldots,L_k\}/l}^k,\mathbf{x}_l^k)$ is named as the first-stage weight. By employing this joint likelihood, parallel partition PF is able to account for the presence of nearby targets in a computationally efficient and generally applicable manner. Recall (9), $p(\mathbf{z}^k|\hat{\mathbf{X}}_{\{1,\ldots,L_k\}/l}^k,\mathbf{x}_l^k)$ can be calculated as

$$p(\mathbf{z}^k|\hat{\mathbf{X}}_{\{1,\ldots,L_k\}/l}^k,\mathbf{x}_l^k) = \prod_{b=1}^{B}\ell(z_b^k;V_b(\hat{\mathbf{X}}_{\{1,\ldots,L_k\}/l}^k,\mathbf{x}_l^k)), \tag{30}$$

Substitution of (29) and (30) into (28), the unnormalized particle weights, which are also referred to as second-stage weight-

s, are computed as

$$\omega_j^k \propto \frac{p(\mathbf{z}^k|\mathbf{X}_j^k)}{\prod_{l=1}^{L_k}\prod_{b=1}^{B}\ell(z_b^k; V_b(\hat{\mathbf{X}}^k_{\{1,\ldots,L_k\}/l}, \mathbf{x}_l^k))}. \tag{31}$$

After normalizing the second-stage weights to sum to one over $j = 1, \ldots, N_p$, the JMPD can be approximated by

$$p(\mathbf{X}^k|\mathbf{Z}^{1:k}) \approx \sum_{j=1}^{N_p} \widetilde{\omega}_j^k \delta(\mathbf{X}^k - \mathbf{X}_j^k), \tag{32}$$

with

$$\widetilde{\omega}_j^k = \frac{\omega_j^k}{\sum_{j=1}^{N_p}\omega_j^k} \tag{33}$$

where $\delta(\cdot)$ is the Dirac delta. Overall, the JMPD can be obtained by recursively implementing (26)-(33). However, the following two problems still need to be addressed:

- *Specific form of likelihood function*: The form of measurement density $\ell(z_b^k; V_b(\mathbf{X}^k))$ need to be specified when computing JMPD. In the existing literature, the densities are usually assumed to be Gaussian or Rayleigh distributed. However, due to the complexity of the practical underwater environment, such statistic models may not be accurate and possibly lead to performance degradation.

- *Unknown and time varying number of targets*: Note that in (26)-(33), the dimension of the multi-target state $\mathbf{X}^k$ in JMPD is always fixed. That means the number of targets is invariant during the filtering process. However, in real-world problems targets may appear or disappear at any time in surveillance area, which means the dimensions of $\mathbf{X}^k$ should also be time-varying rather than fixed.

The above problems will be discussed in the subsequent Sections 3.4 and 3.5, respectively.

3.4. Data Fitting based Likelihood Function Construction

In order to obtain proper forms of the likelihood functions, a data fitting based parameter estimation algorithm is proposed. By comparing the fitness between the empirical distribution of the measured data and candidate distributions with adjustable parameters, the best fitting distribution model with optimized distribution parameters is employed as the specific form of the likelihood function.

3.4.1. Data fitting criteria

Let $z_{b,[i]}, i = 1, 2, \cdots, N_s$ denote a set of measurement samples after beamforming for bearing cell V_b. It should be noted that the statistical characteristics of $\ell(z_b^k; V_b(\mathbf{X}^k))$ are affected by the number $V_b(\mathbf{X}^k)$ of targets in direction cell V_b. Nevertheless, we only need specific models for the two most common cases, namely noise/interference only case ($V_b(\mathbf{X}^k) = 0$) and single target case ($V_b(\mathbf{X}^k) = 1$), since the main challenge of underwater tracking is to accurately differentiate no-target case and target case especially when signal SNR is low. If there are more than one target in bearing cell V_b, we use the model that $\ell(z_b^k; V_b(\mathbf{X}^k) > 1) = \ell(z_b^k; V_b(\mathbf{X}^k) = 1)$. Given N_s independent measurement samples under a specific hypothesis of $V_b(\mathbf{X}^k)$, the empirical cumulative distribution function (ECDF) can be expressed as

$$\hat{F}(z) = \frac{1}{N_s}\sum_{i=1}^{N_s} 1_z(z_{b,[i]}), \tag{34}$$

where $1_z(z_{b,[i]})$ denotes an indicator function

$$1_z(z_{b,[i]}) = \begin{cases} 1, & z_{b,[i]} \le z \\ 0, & z_{b,[i]} > z \end{cases}. \tag{35}$$

To quantify the discrepancy between the ECDF $\hat{F}(z)$ and a certain probability model $F(z)$, the Cramer-von (CV) distance [52] is employed, which describes the fitness between $F(z)$ and the empirical distribution of samples. It is defined as

$$d_{cv}^2 = N_s \int_0^\infty |F(z) - \hat{F}(z)|^2 dF(z). \tag{36}$$

According to [53], the d_{cv}^2 can be simplified as

$$d_{cv}^2 = \frac{1}{12N_s} + \sum_{i=1}^{N_s} |F(z_{b,(i)}) - \frac{2i-1}{2N_s}|^2, \tag{37}$$

where $z_{b,(i)}$ is the i-th sample of the ascending sorted samples, i.e., $z_{b,(1)} \le \cdots z_{b,(i)} \le \cdots \le z_{b,(N_s)}$. Given different distribution functions, the CV distances calculated by (37) are obtained respectively. Hence, the best fitted distribution model and the corresponding distribution parameters can be determined by minimizing the CV distance, i.e., the specific form of likelihood function will be obtained.

Consider n candidates of PDF models $F_i(z, \chi_i), i = 1, 2, ..., n$, where χ_i denotes the parameters of the i-th model. Then the problem of finding a suitable likelihood function becomes the following optimization problem

$$(\hat{i}, \hat{\chi}_{\hat{i}}) = \arg\min_{(i,\chi_i)}(d_{cv}^2(\hat{F}(z), F_i(z, \chi_i))), \tag{38}$$

The optimization of (38) leads to the best fitting PDF from all n candidate PDFs. To solve (38), we first optimize the parameters of each PDF model by minimizing the error defined as indicated above, i.e., minimizes d_{cv}^2 as follows:

$$\hat{\chi}_i = \arg\min_{\chi_i \in \Omega_i}(d_{cv}^2(\hat{F}(z), F_i(z, \chi_i)). \tag{39}$$

where Ω_i is the parameter space of the i-th model and $\hat{\chi}_i$ denotes the estimated model parameters.

Then, based on the estimated parameters of n models, the optimal likelihood function model will be obtained by minimizing CV distance

$$\hat{i} = \arg\min_{i\in\{1,2,\cdots,n\}}(d_{cv}^2(\hat{F}(z), F_i(z, \hat{\chi}_i))). \tag{40}$$

Table 1: CV distances of each models and beamforming methods.

Noise case samples	Rayleigh	Weibull	Gamma	Lognormal
CBF	747.1729	38.0758	0.9786	1.5843
MVDR	917.2526	45.4666	2.5264	3.2504
MUSIC	974.2690	112.3380	13.3290	25.7140
Target case samples	Rayleigh	Weibull	Gamma	Lognormal
CBF	775.8749	33.0082	4.7781	0.8692
MVDR	884.4308	45.8479	2.1380	3.0683
MUSIC	924.6080	42.2134	6.9893	2.8408

3.4.2. *Numerical example*

Assume 40 hydrophones are placed in ULA system, and the distance between each hydrophone is set to $d = 0.5m$. The parameters of frequency segmenting are set as: $N = 2000$ and $\tilde{N} = 100$. The sampling frequency is $4000Hz$. The working frequency is $100 \sim 1000Hz$. Here we consider two sets of measurements samples under two common cases, namely noise (interference) only case ($V_b(\mathbf{X}^k) = 0$) and single target case ($V_b(\mathbf{X}^k) = 1$). For $V_b(\mathbf{X}^k) = 1$, the SNR of the received signal before beamforming is set as -20dB. For $V_b(\mathbf{X}^k) = 0$, only white Gaussian noise is considered. The measurements samples are simulated by first generating signals in multiple frequency segments ($100 \sim 1000Hz$) as represented in (15), and then performing wide-band signal beamforming according to Section 3.2. Then $N_s = 1000$ samples are generated through Monte Carlo (MC) trials. In addition, we consider four classic likelihood distribution models [54]: Rayleigh distribution, Weibull distribution, Gamma distribution and Lognormal distribution.

Based on the above-mentioned two sets of samples and four distribution models, the optimized parameters for each model can be found by solving (38) and (39). To visualize the fitting results, the best fitting CDF curves for all distributions are shown in Fig. 4. It can be seen from the results in Table 1 that the dual-parameter distribution models, such as Gamma and Lognormal distributions, can better describe the statistical characteristics of the spatial spectrum measurements than the usually assumed Rayleigh distribution in terms of much lower CV distances, regardless of the beamforming methods used. This will be seen more clearly in the real-data modeling results in Section 4.2.

Different from the presumed and fixed likelihood models in existing PF-TBD works [25–29], the proposed likelihood construction method learns the underwater environment from real data. In principle, using the proposed method, one can update the distribution model and optimize the model parameters using the latest data, at regular intervals, to ensure that they do not mismatch with the statistical characteristics of actual measurements. It is worth mentioning that although the proposed method is discussed in the context of array sonar tracking, it is a general methodology, and can be applied to other scenarios to address the similar model mismatch problem as well.

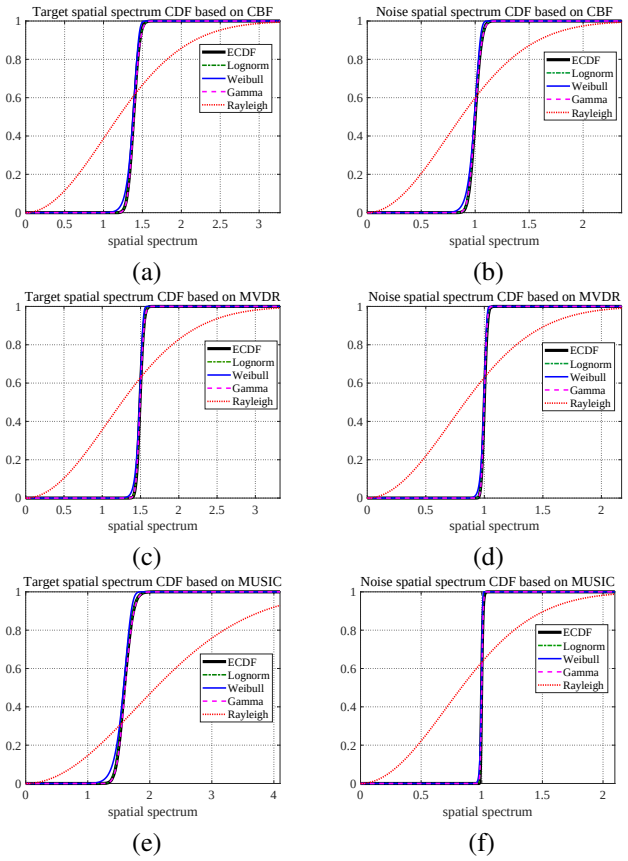

Figure 4: The CDF curves for target and noise cases: (a) and (b) are based on CBF; (c) and (d) are based on MVDR; (e) and (f) are based on MUSIC.

3.5. *Target Initiation and Termination*

Generally the number of targets in track is time-varying due to the birth of new targets, the death of existing targets and the evolution of surviving targets. The common way to handle time-varying number of targets in particle filtering is to define an updated version of dynamic model [39], which assumes that, in addition to the motion model of target states, the evolution of target number also follows a specific probabilistic model, e.g., the $M/M/\infty$ birth-death model. In essence, this kind of probabilistic model characterises the evolution of target number by assuming several prior probabilistic parameters, such as the prior arrival rate of new targets, the expected life time of an existing target. However, in practice it is hard to model the random arrivals and disappearances of targets accurately by several probabilistic parameters.

Here we attempt to circumvent the modeling of the probabilistic characteristics of target number, and propose a simple and intuitive strategy for the initiation and termination of PF-TBD by judging the quality of particle partition for a single target, i.e., $\{\mathbf{x}_{l,j}^k\}_{j=1}^{N_p}$. We use identification (ID) variable [39] $\mathbf{I}^k = \{I_1^k, \ldots, I_{L^k}^k\}$ to label the L^k targets of the multi-target state $\mathbf{X}^k = \left[[\mathbf{x}_1^k]', [\mathbf{x}_2^k]', \ldots, [\mathbf{x}_{L_k}^k]'\right]'$. Note that all the target IDs are distinct. Since we have defined the ID variable, in the rest of the paper, we denote the state of the l-th target as $\mathbf{x}_{I_l^k}^k$.

The ID variable $\mathbf{I}^{k-1}$ can be expressed as the union of the

dying targets with ID variable $\mathbf{D}^k$ and the surviving targets with ID variable $\mathbf{S}^k$,

$$\mathbf{I}^{k-1} = \mathbf{S}^k \cup \mathbf{D}^k. \tag{41}$$

Let $\mathbf{B}^k$ denote the ID variable of new born targets at time k, the ID variable $\mathbf{I}^k$ at time k can be written as

$$\mathbf{I}^k = \mathbf{S}^k \cup \mathbf{B}^k. \tag{42}$$

The basic idea of the proposed strategy is to remove the particle partition of the targets with ID belongs to set $\mathbf{D}^k$ from the multi-target particles $\{\mathbf{X}_j^k\}_{j=1}^{N_p}$, and add the particle partition of the new born targets with ID variable $\mathbf{B}^k$. Then the key is to accurately find out $\mathbf{D}^k$, and build the new particle partition for targets $\mathbf{B}^k$ at each update time.

3.5.1. Target termination strategy

We propose to terminate the trajectory of a certain existing target, say the target with ID I_l^k, by judging the quality of its particle partition i.e., $\{\mathbf{x}_{I_l^k,j}^k\}_{j=1}^{N_p}$. As stated in Section 2.2, the likelihood value for target case and noise case are subtly different and the first-stage particles weights in (30) are directly related to the likelihood functions. Thus, our idea is to judge the death of a certain existing target by evaluating the quality of its first-stage particle weights, i.e., a higher value first-stage particle weight is more likely to indicate the existence of this target. Additionally, to improve the robustness of this judgement, the particle quality for multiple consecutive frames are jointly taken into consideration. This is a common idea adopted in multi-frame detection and tracking method [39, 55]. The MTT particle filter proposed in [39] also adopted similar judgement strategy, while the difference is that the particle filter in [39] uses an updated version of dynamic model with the evolution model of target number.

Let $\Lambda_{I_l^k}$, $l = 1, \ldots, L_k$, denote the sum of multiple frame first-stage particle weights of the target partition with ID I_l^k, and it can be computed as

$$\Lambda_{I_l^k} = \sum_{f=1}^{N_t} \sum_{j=1}^{N_p} p(\mathbf{z}^{k-f+1} | \hat{\mathbf{X}}_{\mathbf{I}^k/I_l^k}^{k-f+1}, \mathbf{x}_{I_l^k,j}^{k-f+1}), \tag{43}$$

where N_p is the number of particles, N_t is the number of consecutive frames considered and $p(\mathbf{z}^k | \hat{\mathbf{X}}_{\mathbf{I}^k/I_l^k}^k, \mathbf{x}_{I_l^k,j}^k)$ denotes the first-stage weight of the j-th particle at time k, see (30). If this target disappears at time k, the value of $\Lambda_{I_l^k}$ should be quite low. Thus the ID variable for the dying targets at time k can be obtained as

$$\mathbf{D}^k = \{I \in \mathbf{I}^{k-1} : \Lambda_I < \eta_d\} \tag{44}$$

where η_d is a pre-define threshold for dying targets. Then the ID variable of the surviving targets is $\mathbf{S}^k = \mathbf{I}^{k-1}/\mathbf{D}^k$.

3.5.2. Target initiation strategy

Since the intensities of generated bearing measurements can provide information on the presence of targets, we adopt a background normalization algorithm [56] to select a number of measurements, whose intensities exceed a certain adaptive threshold, to start the tentative tracks. If the detected measurements are around the existing target tracks or tentative tracks, they are deleted since they are more likely to be generated by the targets in track. The rest of the measurements at time k are collected as $\boldsymbol{\vartheta}^k = \{\vartheta_a^k, a = 1, 2, \ldots, A^k\}$, where ϑ_a^k denotes the bearing value of the a-th measurement and A^k is the number of kept measurements after background normalization. The measurements $\boldsymbol{\vartheta}^k$ are labeled with ID variable $\mathbf{B}_{\text{ten}}^k = \{I_{\text{ten},1}^k, \ldots, I_{\text{ten},A^k}^k\}$ and used to build the prior density of new tentative tracks as

$$p_{\text{ten}}^k(\mathbf{X}_{\mathbf{B}_{\text{ten}}^k}^k) = \prod_{a=1}^{A^k} \mathrm{U}_{\vartheta_a^k}(\theta_{I_{\text{ten},a}^k}^k) \mathrm{V}_0(\dot{\theta}_{I_{\text{ten},a}^k}^k) \tag{45}$$

where $\mathrm{U}_{\vartheta_a^k}(\cdot)$ is a uniform distribution round the bearing value indicated by ϑ_a^k, and $\mathrm{V}_0(\cdot)$ is the distribution of the initial bearing velocities. Then we can draw multi-target particles $\{\mathbf{X}_{\mathbf{B}_{\text{ten}}^k,j}^k\}_{j=1}^{N_p}$ from (45) and propagate forward to compute the JMPD of these tentative tracks using (26)-(33).

Next, we build the new particle partition for newborn targets using the multi-target particles of existing tentative tracks. To ensure the robustness of the initiation strategy, we also adopt the multi-frame judgement similar to that in the termination strategy. Let N_f denote the number of consecutive frames, and $\{\mathbf{X}_{\mathbf{B}_{\text{ten}}^{k-N_f+1},j}^k\}_{j=1}^{N_p}$ denote the multi-target particles of the tentative tracks born at time $k - N_f + 1$. We also propose to select new born tracks by judging the qualities of their particle partitions.

Let $\Upsilon_{I_{\text{ten},a}^{k-N_f+1}}$, $a = 1, \ldots, A^{k-N_f+1}$, denote the sum of multiple frame first-stage particle weights of the target partition with ID $I_{\text{ten},a}^{k-N_f+1}$, and it can be computed as

$$\Upsilon_{I_{\text{ten},a}^{k-N_f+1}} = \sum_{f=1}^{N_f} \sum_{j=1}^{N_p} p(\mathbf{z}^{k-f+1} | \hat{\mathbf{X}}_{\mathbf{B}_{\text{ten}}^{k-N_f+1}/I_{\text{ten},a}^{k-N_f+1}}^{k-f+1}, \mathbf{x}_{I_{\text{ten},a}^{k-N_f+1},j}^{k-f+1}). \tag{46}$$

If this tentative track is deemed to be a new born track at time k, the value of $\Upsilon_{I_{\text{ten},a}^{k-N_f+1}}$ should be quite high. Thus the ID variable for the newborn targets at time k can be obtained as

$$\mathbf{B}^k = \{I \in \mathbf{B}_{\text{ten}}^{k-N_f+1} : \Upsilon_I > \eta_b\} \tag{47}$$

where η_b is a pre-defined threshold for new target birth. The tentative track would be removed if its particle quality fails to pass the threshold test. The particle partition for the newborn targets are extracted from the multi-target particles of tentative tracks, and denoted as $\{\mathbf{X}_{\mathbf{B}^k,j}^k\}_{j=1}^{N_p}$.

3.5.3. Update of the JMPD

According to the aforementioned target initiation and termination strategy, the JMPD is updated by removing the particle partitions with IDs belong to $\mathbf{D}^k$ and adding the particle partitions of new born tracks $\{\mathbf{X}_{\mathbf{B}^k,j}^k\}_{j=1}^{N_p}$. Accordingly, the ID variable is updated as $\mathbf{I}^k = \mathbf{S}^k \cup \mathbf{B}^k$. So far, the PF-TBD method for the passive array sonar system is introduced. A summary of the PF-TBD method is given in Algorithm 1.

Algorithm 1: Summary of the PF-TBD Algorithm

for *each time k* **do**
  - Initiate new tentative tracks by background normalization algorithm.
  for *each track* **do**
    - Sample all the multi-target particles assuming all the tracks survive using (29).
    - Calculate the first-stage weights using (30).
    for *each track of* $\mathbf{I}^{k-1}$ **do**
      - Calculate the sum of weights using (43).
      - Evaluate (44) and terminate the corresponding tracks.
      - Keep the particles of surviving tracks.
    end
    for *each tentative track of* $\mathbf{B}_{ten}^{k-N_f+1}$ **do**
      - Calculate the sum of weights using (46).
      - Initiate the newborn tracks by evaluating (47) and keep the new particles partitions.
    end
  end
  - Update the multi-target particles of JMPD.
  - Resample all the particles.
  - Output the estimated target states $\hat{\mathbf{X}}^k$.
end

3.6. Computational Complexity

According to the previous discussion of the proposed PF-TBD algorithm, the computational complexity mainly consists the following five parts: particle sampling, the first-stage weight calculation, target termination, target initiation and the second-stage weight calculation. Specifically, assuming that all the tracks survive, the complexity for sampling all the multi-target particles is bounded by $O(N_p L_{\text{total}})$, where $L_{\text{total}} = \max_k |\mathbf{I}^{k-1} \cup \mathbf{B}_{\text{ten}}^{k-N_f+1} \cup \cdots \cup \mathbf{B}_{\text{ten}}^{k}|$ with $|\cdot|$ denoting the number of elements in this set. After sampling, we calculate the first-stage weights. The complexity of this operation is $O(N_p L_{\text{total}} B)$ determined by (28), where B denotes the number of bearing cells. For termination operation of certain existing targets, the complexity is contributed by the calculation of (42) and is bounded by $O(N_p L_{\text{exi}} N_t)$, where $L_{\text{exi}} = \max_k |\mathbf{I}^{k-1}|$ denotes the maximum number of existing tracks. Similar with the analysis of target termination, the complexity load of target initiation is bounded by $O(N_p L_{\text{ten}} N_f)$ according to (45), where $L_{\text{ten}} = \max_k |\mathbf{B}_{\text{ten}}^{k-N_f+1}|$ denotes the maximum number of existing tentative tracks. After target termination and initiation, for confirmed tracks, the upper bound of complexity in second-stage weight updating is $O(N_p L_{\text{con}})$, where $L_{\text{con}} = \max_k |\mathbf{S}^k \cup \mathbf{B}^k|$. Note that L_{con} tracks consist the surviving tracks after target termination and the newborn tracks after target initiation. In all, the total computation complexity of PF-TBD is $O(N_p L_{\text{total}}) + O(N_p L_{\text{total}} B) + O(N_p L_{\text{exi}} N_t) + O(N_p L_{\text{ten}} N_f) + O(N_p L_{\text{con}})$.

4. Numerical Results

In this section, both the simulated data and real-world recorded data are used to evaluate the performance of the proposed PF-TBD algorithm in comparison with the Kalman based DBT (KF-DBT). Please note that the KF-DBT is the most widely adopted method in practical underwater acoustic tracking applications, and it is the most relevant reference benchmark for the presented work. For completeness, we also provide results for the Gaussian mixture PHD filter [41]. To guarantee the fairness of the performance comparison, we keep a similar level of false tracks for all three algorithms in the track management strategies and parameter setting.

4.1. Simulation Experiments

Consider a typical underwater bearing-only tracking scenario. The array parameters are set as: $M = 40, d = \frac{\lambda}{2}$ with working frequency $100 \sim 1000Hz$. The propagation speed of acoustic wave is $c = 1531m/s$. The duration of this simulation is $K = 50$ frames. The parameters of frequency segmenting are $N = 2000$ and $\tilde{N} = 100$. The sampling frequency is $4000Hz$. Note that the simulation raw measurements are generated similar to that in the numerical example of Section 3.4. The number of particles used is 400. All the simulation results are averaged over 100 MC runs.

4.1.1. Performance comparison for three different beamforming methods

As is shown in Fig. 5, we first consider a simple scenario where a single emitter is moving in the surveillance area from $-90°$ to $90°$. For each of the three beamforming methods described in Section III, the BTRs after beamforming are shown in Fig. 6. It can be seen that the outputted power spectrums of CBF and MVDR are more robust than that of MUSIC when target SNR is low, while MUSIC can provide higher quality power spectrum when SNR is high. Note that the mentioned SNR in Fig. 6 is the SNR of received signal before beamforming.

Next, these generated BTR measurements are directly used as the inputs of the proposed PF-TBD algorithm. Both the root mean square error (RMSE) and the probability of detection (P_d) are employed as the performance evaluation metrics, and a target is deemed to be successfully tracked if the estimated direction error is less than 4°. As shown in Fig. 7, both metrics demonstrate that the CBF and MVDR are better beamforming

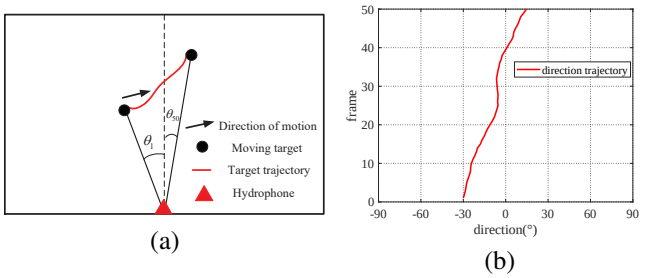

(a) (b)

Figure 5: (a) The schematic diagram of simulation scene. (b) The real target trajectory in direction.

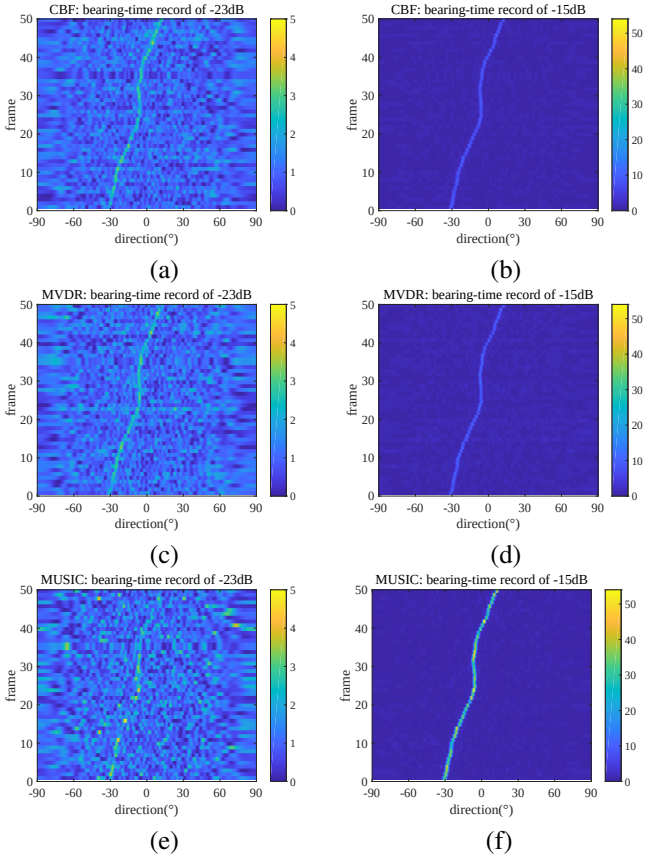

Figure 6: The bearing-time record of three beamforming method. The SNR of the received array signal is -23dB in (a) (c) (e), and -15dB in (b) (d) (f).

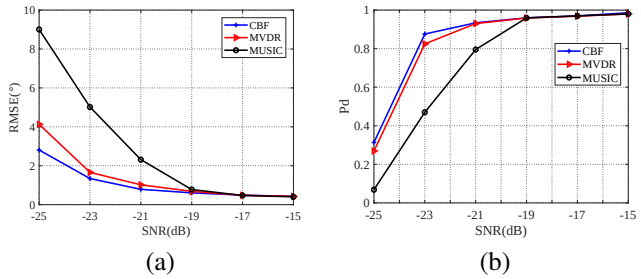

Figure 7: The RMSE and P_d curves of the proposed PF-TBD algorithm are plotted against SNR for the three beamforming methods. (a) RMSE. (b) Probability of detection.

choices than MUSIC due to their robust performance in low SNR conditions. In addition, the performance of CBF slightly outperforms MVDR despite its lower computational complexity. Thus, we adopt CBF as the beamforming choice in the subsequent simulation studies.

4.1.2. MTT performance

Here we consider a complex scenario with five moving emitters and cross tracks. To examine the capability of tracking targets with time-varying existence, two targets are set to born at the 15-th frame and one target disappears at 36-th frame. The parameter setting for target initiation and termination modules are: $N_f = 3$ and $N_t = 3$. The process noise intensity in the

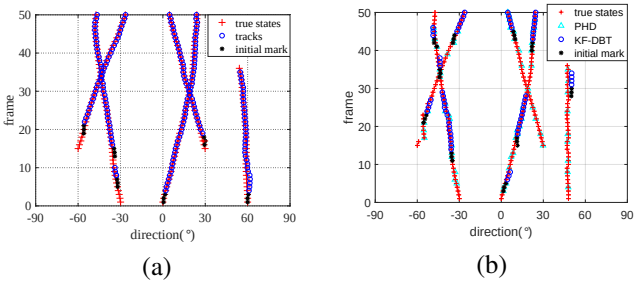

Figure 8: The tracking results of a single MC run where the SNR of the received array signal is −23dB: (a) PF-TBD, (b) KF-DBT vs PHD.

dynamic model (12) is set as $\kappa = 1°/s^2$. The comparison results with the KF-DBT method and the PHD filter are also given. The inputs of the KF-DBT and PHD filter are the thresholded angular detections, and the corresponding observation model is assumed to be linear and Gaussian with standard deviation of the measurement noise $\sigma = 1°$. Besides, the target survival probability is set as $P^S = 0.98$ in PHD filter. The detection probabilities are set to be $P^D = 0.98$ for SNR=−19 dB, $P^D = 0.90$ for SNR=-21 dB, and $P^D = 0.80$ for SNR= −23 dB. For target birth, similar with [61], the birth information is assumed to be known as a prior. The pruning parameters for PHD is $T_p = 1 \times 10^{-5}$ and the maximum number of targets that the PHD filter handles at one time is $N_{max} = 100$.

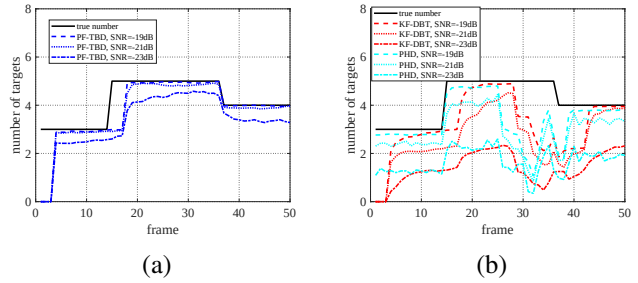

Figure 9: The number of successfully tracked targets are plotted against frame time for three methods: (a) PF-TBD, (b) KF-DBT vs PHD.

The tracking results of a single MC run under SNR= −23 dB are first shown in Fig. 8. We can observe that the trajectories returned by the KF-DBT and PHD filter are quite incomplete compared with that of PF-TBD in low SNR condition. The curves of the successfully tracked targets are plotted against frame time in Fig. 9. It can be seen that the proposed PF-TBD can deliver better detection performance compared to the KF-DBT and PHD methods especially when SNR is low.

Next, the generalized optimal subpattern assignment (GOSPA) [57, 58] metric is employed to further study the tracking performance of the three algorithms. As an extension of the OSPA [57] metric, the GOSPA metric can penalize localization errors for detected targets and the errors due to missed and false targets. The the GOSPA results with parameters $\alpha = 2$, $p = 1$, $c = 4$ are shown in Fig. 10, including the total tracking error, the localisation error, the missed detection error and the false detection error. It can be seen in Fig. 10 that PF-TBD also provides better tracking performance es-

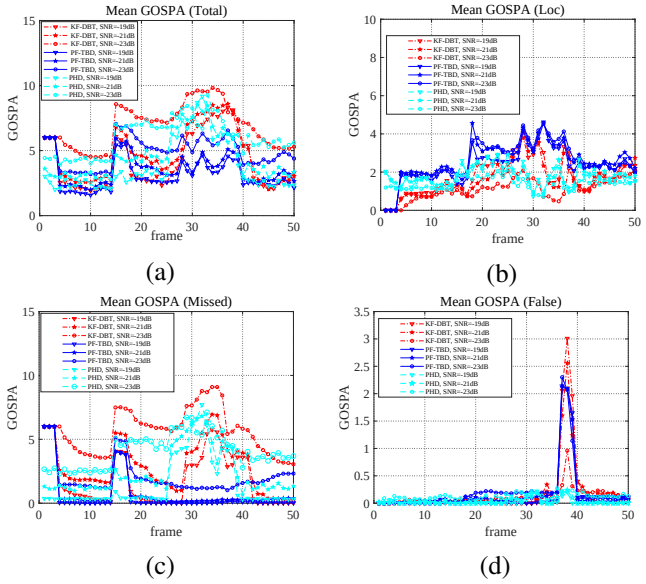

Figure 10: The GOSPA curves are plotted against frame time for both methods. (a) the total error, (b) the localisation error, (c) the missed detection error, (d) the false detection error.

Table 2: Optimal parameters and CV distance of each model for the real data set.

Models	Rayleigh	Weibull	Gamma	Lognormal
Target	5.3451	5.9714,6.6013	53.1921,0.1213	1.8550,0.1898
CV	15.1238	2.4868	1.9541	0.0621
Model	Rayleigh	Weibull	Gamma	Lognormal
Noise	1.0619	9.0999,1.1614	53.7485,0.0215	0.1529,0.1898
CV	101.8652	69.7351	31.1284	18.4450

pecially when target SNR is low. Besides, the tracking performance of the PHD filter is roughly similar to the KF-DBT. In contrast to the PHD filter, PF-TBD and KF-DBT require several frames to confirm new born and disappeared targets. This is because the standard PHD filter [41] is a multi-target state estimator which only reports the multi-target state estimation results at each frame time.

4.2. Real-world Recorded Data

In this part, the proposed PF-TBD algorithm is further verified using a set of real experimental data recorded from a towed passive uniform linear array. The data set was collected in a shallow sea and the received acoustic signals were the noises generated by the moving ships. The received raw array signals are processed according to Sections 3.1 and 3.2. The generated BTR of this data set for the considered time span is depicted in Fig. 11 (a) and constitutes the input to the filter. It can be seen that six targets are moving in the surveillance area and the two targets around $40^\circ \sim 60^\circ$ are very weak. Also, it is worth mentioning that the measurements in the directions between $-90^\circ \sim -60^\circ$ are not taken into account, since these measurements are generated by the towed ship itself. As shown in Fig. 11 (b), these noise measurements generated by towed ship are eliminated after background normalization.

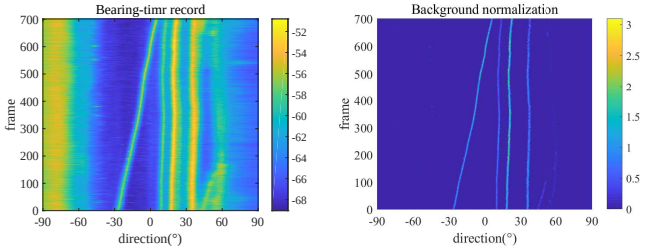

Figure 11: (a) The raw BTR map of the recorded real data. (b) The BTR map after background normalization processing.

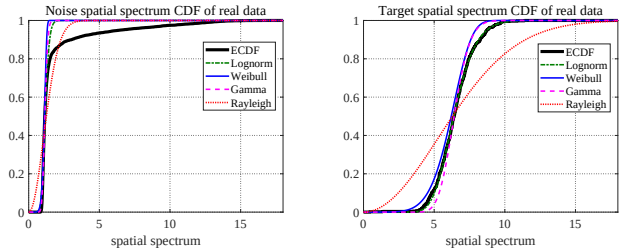

Figure 12: The CDF fitting results of the real data. (a) noise only samples, (b) target related samples.

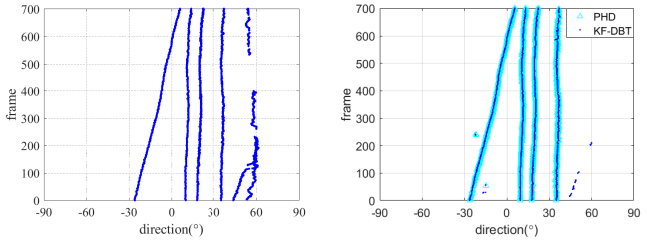

Figure 13: The tracking results of the real data. (a) PF-TBD, (b) KF-DBT vs PHD.

To obtain an accurate likelihood function, the data fitting based parameters estimation algorithm is first employed. The fitting results are shown in Fig. 12 and Table 2. It can be seen clearly that Lognormal model is the best fitting one. Then, the tracking results, depicted in Fig. 13, show that the proposed PF-TBD algorithm can track the two weak targets (targets in $40^\circ \sim 60^\circ$) much more accurately than KF-TBD and PHD filter.

5. Conclusion

This work considers the underwater tracking of an unknown and time-varying number of moving acoustic emitters using passive array sonar systems. To enhance the tracking performance of low SNR targets, we proposed a complete particle filter track-before-detect (PF-TBD) procedure especially developed for passive array sonar systems. The received wideband array acoustic signals were directly used as the inputs of the proposed PF-TBD to avoid the information loss during the

thresholding process. To better model the statistical characteristics of the spectrum measurements after the beamforming of the acoustic signals, a data fitting based parameter estimation algorithm was proposed to obtain a suitable likelihood function. Particle filter was employed to propagate forward the joint multi-target probability density. The trajectory initiation and termination strategies were also integrated into the filtering process to accommodate the time-varying number of targets. The efficacy of the proposed PF-TBD method was demonstrated both in simulation and on collected real-world data. In the future, we will extend the proposed method with RFS theory based TBD methods [59, 60] and also consider the information fusion among multiple passive array sonar systems [61–63].

[1] G. C. Carter, "Time delay estimation for passive sonar signal processing," *IEEE Transactions on Acoustics Speech and Signal Processing*, vol. 29, no. 3, pp. 463–470, 1981.

[2] J. Luo, H. Ying and L. Fan, "Underwater acoustic target tracking: A Review," *Sensors*, vol. 18, no. 2, 2018.

[3] B. Xerri, J. F, Cavassilas and B. Borloz, "Passive tracking in underwater acoustic," *Signal Processing*, vol. 82, no. 8, pp. 1067–1085, 2002.

[4] S. G. Lemon, "Towed-array history, 1917-2003," *IEEE Journal of Oceanic Engineering*, vol. 29, no. 2, pp. 365–373, 2004.

[5] D. H. Johnson and S. R. Degraaf, "Improving the resolution of bearing in passive sonar arrays by eigenvalue analysis," *IEEE Transactions on Acoustics Speech and Signal Processing*, vol. 30, no. 4, pp. 638–647, 1981.

[6] Y. Bar-Shalom, T. Kirubarajan and X. R. Li, *Estimation with Applications to Tracking and Navigation*, Wiley, 2001.

[7] A. Farina, "Target tracking with bearings-only measurements," *Signal Processing*, vol. 78, no. 1, pp. 61–78, 1999.

[8] S. Blackman and R. Popoli, *Design and Analysis of Modern Tracking Systems*, Artech House, 1999.

[9] M. Mallick, M. Morelande and L. Mihaylova, "Angle-only filtering in three dimensions," in *Integrated Tracking, and Classification, and Sensor Management: Theory and Applications*, Wiley/IEEE, pp. 3–42, 2012.

[10] B. A. Yocom, B. R. La Cour, and T. W. Yudichak, "A Bayesian approach to passive sonar detection and tracking in the presence of interferers," *IEEE Journal of Oceanic Engineering*, vol. 36, no. 3, pp. 386–405, 2011.

[11] D. Musicki, "Multi-target tracking using multiple passive bearings-only asynchronous sensors," *IEEE Transactions on Aerospace and Electronic Systems*, vol. 44, no. 3, pp. 1151–1160, 2008.

[12] S. K. Rao, "Modified gain extended Kalman filter with application to bearings-only passive manoeuvring target tracking," *IEE Proceedings-Radar, Sonar and Navigation*, vol. 152, no. 4, pp. 239–244, 2005.

[13] V. J. Aidala, "Kalman filter behavior in bearings-only tracking applications," *IEEE Transactions on Aerospace and Electronic Systems*, vol. 15, no. 1, pp. 29–39, 2007.

[14] S. Sadhu, S. Mondal and M. Srinivasan, " Sigma point Kalman filter for bearing only tracking," *Signal Processing*, vol. 86, no. 12, pp. 3769–3777, 2006.

[15] T. Fortmann, Y. Bar-Shalom, and M. Scheffe, "Sonar tracking of multiple targets using joint probabilistic data association," *IEEE Journal of Oceanic Engineering*, vol. 8, no. 3, pp. 173–184, 1983.

[16] F. El-Hawary, F. Aminzadeh and G. A. N. Mbamalu, "The generalized Kalman filter approach to adaptive underwater target tracking," *IEEE Journal of Oceanic Engineering*, vol. 17, no. 1, pp. 129–137, 1992.

[17] D. R. Kumar, S. K. Rao, K. P. Raju, "A novel stochastic estimator using pre-processing technique for long range target tracking in heavy noise environment," *Optik-International Journal for Light and Electron Optics*, vol. 127, no. 10, pp. 4520–4530, 2016.

[18] M. Mallick, M. Morelande and L. Mihaylova, "Comparison of angle-only filtering algorithms in 3D using Cartesian and modified spherical coordinates," in *2012 15th International Conference on Information Fusion*, July 2012, pp. 1392–1399.

[19] J. Georgy, A. Noureldin, "Unconstrained underwater multi-target tracking in passive sonar systems using two-stage PF-based technique," *International Journal of Systems Science*, vol. 45, no. 3, pp. 439–455, 2014.

[20] F. Gustafsson, F. Gunnarsson and N. Bergman, "Particle filters for positioning, navigation, and tracking," *IEEE Transactions on Signal Processing*, vol. 50, no. 2, pp. 425–437, 2002.

[21] J. Candy, "Bootstrap particle filtering," *IEEE Signal Processing Magazine*, vol. 24, no. 4, pp. 73–85, 2007.

[22] M. Orton, W. Fitzgerald, "A Bayesian approach to tracking multiple targets using sensor arrays and particle filters," *IEEE Transactions on Signal Processing*, vol. 50, no. 2, pp. 516–223, 2002.

[23] D. Elsharkawi, A. Ali and C. M. Evans, "A review of concealed weapon detection and research in perspective," *IEEE International Conference on Networking*, pp. 443–448, 2007.

[24] B. Ristic, M. Arulampalam, and N. Gordon, *Beyond the Kalman Filter: Particle Filters for Tracking Applications*, Norwood, MA: Artech House, 2004.

[25] Y. Boers and J. N. Driessen, "Multitarget particle filter track before detect application," *IEE Proceedings - Radar Sonar and Navigation*, vol. 151, no. 6, pp. 351–357, 2004.

[26] D. J. Salmond and H. Birch, "A particle filter for track-before-detect," *American Control Conference*, pp. 3755–3760, 2001.

[27] M. Morelande and B. Ristic, "Signal-to-noise ratio threshold effect in track before detect," *IET Radar Sonar and Navigation*, vol. 3, no. 6, pp. 601–608, 2010.

[28] C. Kreucher and B. Shapo, "Multitarget detection and tracking using multisensor passive acoustic data," *IEEE Journal of Ocanic Engineering*, vol. 36, no. 2, pp. 205–218, 2011.

[29] A. A. Saucan, C. Sintes, T. Chonavel, and J. M. Le Caillec, "Robust, track before detect particle filter for bathymetric sonar application," in *2014 17th International Conference on Information Fusion*, July 2014, pp. 1–7.

[30] L. Xu, C. Liu and W. Yi, "A particle filter based track-before-detect procedure for towed passive array sonar system," *IEEE Radar Conference*, pp. 1460–1465, 2017.

[31] M. Fallon and S. Godsill, "Acoustic source localization and tracking using track before detect," *IEEE Transactions on Audio, Speech, and Language Processing*, vol. 18, no. 6, pp. 1228–1242, 2010.

[32] F. Lehman, "Recursive Bayesian filtering for multitarget track-before-detect in passive radars," *IEEE Transactions on Aerospace and Electronic Systems*, vol. 48, no. 3, pp. 2458–2480, 2012.

[33] C. Kreucher, K. Kastella, and A. O. Hero, "Multitarget tracking using the joint multitarget probability density," *IEEE Transactions on Aerospace and Electronic Systems*, vol. 41, no. 4, pp. 1396–1414, 2005.

[34] M. R. Morelande, C. M. Kreucher, and K. Kastella, "A Bayesian approach to multiple target detection and tracking," *IEEE Transactions on Signal Processing*, vol. 55, no. 5, pp. 1589–1604, 2007.

[35] R. P. S. Mahler, B. T. Vo and B. N. Vo, "CPHD filtering with unknown clutter rate and detection profile,"*IEEE Transactions on Signal Processing*, vol. 59, no. 8, pp. 3497-3513, 2011.

[36] B. T. Vo, B. N. Vo and et al, "Robust multi-Bernoulli filtering," *IEEE Journal of Selected Topics in Signal Processing*, vol. 7, no. 3, pp. 399-409, 2013.

[37] Y. Punchihewa, B. T. Vo, B. N. Vo and et al, "Multiple object tracking in unknown backgrounds with labeled random finite sets," *IEEE Transactions on Signal Processing*, vol. 66, no. 11, pp. 3040-3055, 2017.

[38] S. Singh, N. Whiteley, and S. Godsil, "An approximate likelihood method for estimating the static parameters in multi-target tracking models," Dept. Eng. Univ. Cambridge, Cambridge, U.K., Tech. Rep. CUED/F- INFENG/TR.606, 2009.

[39] Á. F. García-Fernández, J. Grajal, and M. R. Morelande, "Two-layer particle filter for multiple target detection and tracking," *IEEE Transaction on Aerospace and Electronic System*, vol. 49, no. 3, pp. 1569–1588, 2013.

[40] Á. F. García-Fernández and M. R. Morelande, "Explicit filtering equations for labelled random finite sets," 2015 International Conference on Control, Automation and Information Sciences (ICCAIS), Changshu, 2015, pp. 349-354.

[41] B.-T. Vo and M. Wing-Kin, "The Gaussian Mixture Probability Hypothesis Density Filter," *IEEE Transactions on Signal Processing*, vol. 54, pp. 4091-4104, 2006.

[42] H. Krim and M. Viberg, "Two decades of array signal processing research: the parametric approach," *IEEE Signal Processing Maganize*, vol. 13, no. 4, pp. 67–94, 1996.

[43] G. Su and M. Morf, "The signal subspace approach for multiple wideband emitter location," *IEEE Transactions on Acoustics, Speech and Sig-*

nal Processing, vol. 31, no. 6, pp. 1502–1522, 1983.

[44] H. Wang and M. Kaveh, "Coherent signal-subspace processing for the detection and estimation of angles of arrival of multiple wide-band sources," *IEEE Transactions on Acoustics, Speech and Signal Processing*, vol. 33, no. 4, pp. 823–831, 1985.

[45] A. El-Keyi and T. Kirubarajan, "Adaptive beamspace focusing for direction of arrival estimation of wideband signals," *Signal Processing*, vol. 88, no. 8, pp. 2063–2077, 2008.

[46] M. S. Bartlett, "Smoothing periodograms from time-series with continuous spectra," *Nature*, vol. 161, pp. 686–687, 1948.

[47] J. Capon, "High-resolution frequency-wavenumber spectrum analysis," *Proceedings of the IEEE*, vol. 57, no. 8, pp. 1408–1418, 1969.

[48] R. O. Schmidt, "Multiple emitter location and signal parameters estimation," *IEEE Transactions on Antennas and Propagation*, vol. 34, no. 3, pp. 276–280, 1986.

[49] M. S. Arulampalam, S. Maskell, N. Gordon, and T. Clapp, "A tutorial on particle filters for online nonlinear/non-Gaussian Bayesian tracking," *IEEE Transactions on Signal Processing*, vol. 50, no. 2, pp. 174–188, 2002.

[50] W. Yi, M. R. Morelande, L. J. Kong, and J. Y. Yang, "A computationally efficient particle filter for multitarget tracking using an independence approximation," *IEEE Transactions on Signal Processing*, vol. 61, no. 4, pp. 843–856, 2013.

[51] M. K. Pitt and N. Shephard, "Filtering via simulation: auxiliary particle filters," *Publications of the American Statistical Association*, vol. 94, pp. 590–599, Jun. 1999.

[52] T. W. Anderson, "On the distribution of the two-sample cramr-von mises criterion," *Annals of Mathematical Statistics*, vol. 34, no. 1,pp. 1148–1159, 1962.

[53] F. Laio, "Cramer-von Mises and Anderson-darling goodness of fit tests for extreme value distributions with unknown parameters," *Water Resources Research*, vol. 40, no. 9, pp. 333–341, 2004.

[54] M. I. Skolnik, *Introduction to Radar System*, 3d ed., McGraw-Hill, New York, 2001.

[55] W. Yi, M. Morelande, L. Kong, and J. Yang, "An efficient multi-frame track-before-detect algorithm for multi-target tracking," *IEEE Journal of Selected Topics in Signal Processing*, vol. 7, no. 3, pp. 421–434, 2013.

[56] Q. Li, X. Pan, and Y. Li, "A new algorithm of background equalization," *Acta Acustica*, 2000.

[57] D. Schuhmacher, B. T. Vo and B. N. Vo, "A consistent metric for performance evaluation of multi-object filters," *IEEE Transactions on Signal Processing*, vol. 56, no. 8, pp. 3447–3457, 2008.

[58] A. S. Rahmathullah, Á. F. García-Fernández and L. Svensson, "Generalized optimal sub-pattern assignment metric," in *2017 20th International Conference on Information Fusion*, July 2017.

[59] S. Li, W. Yi, R. Hoseinnezhad, B. Wang, and L. Kong, "Multiobject tracking for generic observation model using labeled random finite sets," *IEEE Transactions on Signal Processing*, vol. 66, no. 2, pp. 368–383, 2019.

[60] Á. F. García-Fernández, "Track-before-detect labeled multi-bernoulli particle filter with label switching", *IEEE Transactions on Aerospace and Electronic Systems*, vol. 52, no. 5, pp. 2123–2138, 2017.

[61] W. Yi, S. Li, B. Wang, R. Hoseinnezhad, and L. Kong, "Computationally Efficient Distributed Multi-sensor Fusion with Multi-Bernoulli Filter," *arXiv preprint arXiv:1906.07991,* 2019.

[62] S. Li, G. Battistelli, L. Chisci, W. Yi, B. Wang, and L. Kong, "Computationally Efficient Multi-Agent Multi-Object Tracking With Labeled Random Finite Sets," *IEEE Transactions on Signal Processing*, vol. 67, no. 1, pp. 260–275, 2019.

[63] S. Li, W. Yi, R. Hoseinnezhad, G. Battistelli, B. Wang, and L. Kong, "Robust distributed fusion with labeled random finite sets," *IEEE Transactions on Signal Processing*, vol. 66, no. 2, pp. 278–293, 2019.